Triple-differential cross sections for inner-shell electron-impact ionization of carbon

Xiang-Fu Jia,* Ming-Hai Liu, Shi-Yan Sun, and Yuan Wu
College of Physics and Information Engineering, Institute of Modern Physics, Shanxi Teachers University, Linfen, Shanxi 041004, People's Republic of China
(Received 28 April 2003; published 10 June 2004)

Triple-differential cross sections (TDCS) have been calculated for the *K*-shell ionization of carbon atom by fast electron impact for highly asymmetric kinematics. In the present calculation the three Coulomb two-body interaction, the dynamic screening modification of these interactions and the correlation in the final channel, the screening effect of the multielectron target, and the distortion of Coulomb force in the initial channel have been taken into account. Results are compared with the relative measurement performed on the C_2H_2 molecule as target. The present TDCS is found to be in better accord with experiment.

DOI: 10.1103/PhysRevA.69.062707 PACS number(s): 34.80.Dp, 34.80.Gs

I. INTRODUCTION

The interaction of the fast moving charged particles with inner-shell electron plays an important role in collision spectroscopy. It is therefore of great interest to study the characteristics of deep inelastic atomic collisions which result in the production of inner-shell vacancies. Particularly the *K*-shell ionization cross section of atoms finds important application in Auger-electron spectroscopy, electron energy-loss spectroscopy, etc. By virtue of the electron-electron coincidence experiments, it has now become feasible to study the collision dynamics with detailed information by measuring the triple-differential cross sections (TDCS) of an ionization process. A number of TDCS measurements have been performed for inner-shell ionizations of different neutral atoms [1–5].

On the theoretical side most of the calculations on inner-shell ionization refer to plane-wave Born approximation which however fails to describe the characteristic features of the experiment. Thus, first Born approximation is not adequate for such process and as such a higher-order calculation or a distorted-wave theory is needed [6]. Botero and Macek [7] have performed a Coulomb-Born calculation of the TDCS for inner-shell of electron-impact ionization of carbon following the experiment to Avaldi, Camilloni, and Stefani [1] who measured the inner-shell ionization cross section of C $\sigma 1s$ orbital in the molecule C_2H_2 for asymmetric geometry. However, the authors [7] in their theoretical work neglected the final-state correlation between the scattered electron and the electron ejected from the *K* shell of carbon atom. Nath, Biswas, and Sinha [8] have considered this continuum-continuum correlation effect by choosing the final state as the three-Coulomb-wave function (3C) of Brauner, Briggs, and Klar [9] while the incident electron is assumed to be deflected by the atomic field of the atom and hence a Coulomb wave is considered for it, the latter being also considered by Botero and Macek [7] but in a slightly different way. The 3C approach is a nonperturbational method, which treats all two-body interactions on equal footing. However, it does not account for coupling between each of the two-body subsystems to the third particles; i.e., within the 3C model the charged particles move due to their mutual two-body potential, which is quite different from the total potential [10].

In the present paper, the TDCS have been calculated for the inner-shell ionization from the 1*s* shell of carbon by considering this screening effect of the multielectron target. The electron exchange effect between the scattered and the ejected *K*-shell electron has been taken into account. The difference between a plane wave and a Coulomb wave in the initial channel is also investigated. Results are compared with the relative measurement performed on the C_2H_2 molecule as target [1] and the theoretical 3C, dynamic screening 3C (DS3C), and Coulomb-Born approximation (CBA) results. The qualitative agreement of the present results with the experiment by Avaldi, Camilloni, and Stefani is better than that of other theoretical results, particularly in respect to the recoil peak position. Atomic units (a.u.) are used unless otherwise specified.

II. THEORETICAL MODEL

We consider the following inner-shell single ionization $(e,2e)$ process:

$$e^- + \mathrm{C}(1s^2 2s^2 2p^2) \rightarrow 2e^- + \mathrm{C}^+(1s 2s^2 2p^2). \qquad (1)$$

To describe the multielectron target containing $N+1$ electrons, a simplified model has been adopted where the set of *N* electrons that are not ionized is considered to be "passive" such that their interactions with the active electron do not contribute to the ionization process. It is also assumed that these passive electrons occupy the same orbital before and after the collision process. As a consequence of this simplification, an explicit introduction of the dynamics of *N* passive electrons into the transition amplitudes for the process, Eq. (1), is avoided and the many-electron problem is reduced to a three-body one [11]. Therefore, we approximate the total Hamiltonian of the system by an electron in an effective Coulomb field,

*Email address: jiaxf@dns.sxtu.edu.cn

$$H = H_0 - \frac{Z_T}{r_1} - \frac{Z_T}{r_2} + \frac{1}{r_{12}}, \tag{2}$$

Z_T being the screened charge of target, chosen such that it gives the experimental binding energy ϵ_i [1], i.e., $Z_T = (-2\epsilon_i)^{1/2}$. $\mathbf{r}_1$ and $\mathbf{r}_2$ are the position vectors of the incoming electron 1 and the bound electron 2, respectively, with respect to the target nucleus, $\mathbf{r}_{12} = \mathbf{r}_1 - \mathbf{r}_2$. H_0 in Eq. (2) is the full kinetic-energy operator given by

$$H_0 = -\frac{1}{2}\nabla_1^2 - \frac{1}{2}\nabla_2^2. \tag{3}$$

The initial channel wave function Ψ_i^+ satisfies the equation

$$\left[H_0 - \frac{Z_T}{r_2} - \frac{Z_T - 1}{r_1}\right]\Psi_i^+ = E_0\Psi_i^+, \tag{4}$$

where

$$\Psi_i^+ = \frac{1}{(2\pi)^{3/2}}\exp\left(\frac{\pi\alpha_i}{2}\right)\Gamma(1 - i\alpha_i) \times \exp(i\mathbf{k}_i \cdot \mathbf{r}_1)\,{}_1F_1\,(i\alpha_i; 1; i(k_i r_1 - \mathbf{k}_i \cdot \mathbf{r}_1))\,\phi_i(\mathbf{r}_2), \tag{5}$$

where $\alpha_i = (Z_T - 1)/k_i$ and $E_0 = k_i^2/2 + \epsilon_i$, $\mathbf{k}_i$ being the initial momentum of the incident electron, and ϕ_i is the initial hydrogenlike bound-state wave function of carbon atom,

$$\phi_i(\mathbf{r}_2) = \left(\frac{Z_T^3}{\pi}\right)^{1/2}\exp(-Z_T r_2). \tag{6}$$

The perturbation V_i in the initial channel which is the part of the total interaction nondiagonalized in the initial state is given by

$$V_i = \frac{1}{r_{12}} - \frac{1}{r_1}. \tag{7}$$

It is evident from Eq. (7) that the perturbation V_i vanishes asymptotically (for $r_1 \to \infty$ and r_2 is finite).

The final-state wave function Ψ_f^- is chosen as

$$\Psi_f^-(\mathbf{r}_1, \mathbf{r}_2) = (2\pi)^{-3}\exp(i\mathbf{k}_1 \cdot \mathbf{r}_1 + i\mathbf{k}_2 \cdot \mathbf{r}_2) \times \prod_j N_{j1}F_1(i\alpha_j; 1; -i(k_j r_j + \mathbf{k}_j \cdot \mathbf{r}_j)), \tag{8}$$

where $j \in \{1, 2, 12\}$, $\mathbf{k}_1$ and $\mathbf{k}_2$ are the momenta of the scattered and the ejected electron, respectively, and $\mathbf{k}_{12}$ is defined as $\mathbf{k}_{12} = (\mathbf{k}_1 - \mathbf{k}_2)/2$, whereas its conjugate coordinate is given by $\mathbf{r}_{12} = \mathbf{r}_1 - \mathbf{r}_2$. N_j, $j \in \{1, 2, 12\}$ are normalization constants which can be given by

$$N_j = \exp(-\alpha_j\pi/2)\Gamma(1 - i\alpha_j). \tag{9}$$

Also, $\alpha_j, j \in \{1, 2, 12\}$ are Sommerfeld parameters. The assumption that the three-body system consists of three spatially independent two-body systems leads to the representation of the Sommerfeld parameters in the 3C model [9] as

$$\alpha_1 = -Z_T/k_1, \quad \alpha_2 = -Z_T/k_2, \quad \alpha_{12} = 1/2k_{12}. \tag{10}$$

The 3C wave function Ψ_f^- in Eq. (8) satisfies the asymptotic three-body boundary condition for an ionization process.

Although this approximation has been very successful in describing angular distributions of ionized electrons, for both electron impact and photoionization [9,12], it suffers from several deficiencies. The most serious of these concerns the absolute value of cross sections obtained for low total energy of the continuum electron. In this case it appears that the absolute values are much too low. The physical origin of this behavior is that the two-body electron-electron wave function takes no account of the screening of the electron-electron interaction by the nucleus, even when the two electrons move slowly on opposite sides of the nucleus, such as near threshold. Berakdar and Briggs [10] proposed a strategy to correct this problem, involving the introduction of effective charges in the 3C wave function. The modified Sommerfeld parameters are given by [13]

$$\gamma_1 = Z_1/k_1, \quad \gamma_2 = Z_2/k_2, \quad \gamma_{12} = Z_{12}/2k_{12}, \tag{11}$$

where the functions occurring in Eq. (11) are defined as

$$Z_{12}(\mathbf{k}_1, \mathbf{k}_2) = [1 - (fg)^2 a^{b_1}]a^{b_2},$$

$$Z_1(\mathbf{k}_1, \mathbf{k}_2) = -Z_T + (1 - Z_{12})\frac{k_1^{1+a}}{(k_1^a + k_2^a)|\mathbf{k}_1 - \mathbf{k}_2|},$$

$$Z_2(\mathbf{k}_1, \mathbf{k}_2) = -Z_T + (1 - Z_{12})\frac{k_2^{1+a}}{(k_1^a + k_2^a)|\mathbf{k}_1 - \mathbf{k}_2|},$$

$$f = [3 + \cos^2(4\alpha)]/4, \quad \tan\alpha = k_1/k_2,$$

$$g = |\mathbf{k}_1 - \mathbf{k}_2|/(k_1 + k_2),$$

$$b_1 = 2k_1k_2\cos(\theta_{12}/2)/(k_1^2 + k_2^2),$$

$$b_2 = g^2\left[-0.5 + \frac{1}{4}\left(\sqrt{\frac{100Z_T - 9}{4Z_T - 1}} - 1\right)\right],$$

$$a = \frac{E_1 + E_2}{E_0}.$$

Here E is measured in atomic units. The interelectronic relative angle $\theta_{12} = \cos^{-1}\hat{\mathbf{k}}_1 \cdot \hat{\mathbf{k}}_2$. This modification of the 3C wave function has removed its major deficiency (namely, the inability to predict absolute cross sections near threshold) and significantly improved the agreement with the detailed shape of angular distributions.

However, for the present case of high incident energy and inner-shell ionization of the multielectron target, it is suggested to completely subsum the interaction of the electron with other particles into effective screened nucleus. We refer to it as S3C method.

To this end we employ the same ideas as in Refs. [10,14]. The new Sommerfeld parameters β_i are introduced simply by a linear transformation from the original set α_i, i.e.,

$$\beta_i = \sum_{j=1}^{3} A_{ij}\alpha_j, \tag{12}$$

where the nine coefficients $A_{ij} \in R$ and $i=1$, 2, or 12 designate the two-body interaction of the two electrons with the residual ion and the electron-electron interaction, respectively. And the condition

$$\beta_1 + \beta_2 + \beta_{12} = \alpha_1 + \alpha_2 + \alpha_{12} \tag{13}$$

should be satisfied. On the other hand, for the inner-shell ionization of a multielectron target (carbon), the effective charge of the ion seen by one electron reduces as the momentum of this one increases due to the screening of the other electrons. Then the effective charge of ion seen by the two outgoing electrons should be in the range $1 < Z_{eff} \leqslant Z_T$, and $Z^i_{eff} \to Z_T$ as $k_j \to \infty$ $(i \neq j; i,j = 1,2)$. based on this consideration, it is readily established that these conditions are satisfied by

$$\beta_1 = \frac{-Z_T + \frac{k_1}{k_{12}}\left[\frac{1}{2}\arccos(\hat{\mathbf{k}}_1 \cdot \hat{\mathbf{k}}_2)\right]^2\left(1 - \frac{|k_1 - k_2|}{4k_{12}}\right)}{k_1}, \tag{14}$$

$$\beta_2 = \frac{-Z_T + \frac{k_2}{k_{12}}\left[\frac{1}{2}\arccos(\hat{\mathbf{k}}_1 \cdot \hat{\mathbf{k}}_2)\right]^2\left(1 - \frac{|k_1 - k_2|}{4k_{12}}\right)}{k_2}, \tag{15}$$

$$\beta_{12} = \frac{1 - 4\left[\frac{1}{2}\arccos(\hat{\mathbf{k}}_1 \cdot \hat{\mathbf{k}}_2)\right]^2\left(1 - \frac{|k_1 - k_2|}{4k_{12}}\right)}{2k_{12}}. \tag{16}$$

Here new Sommerfeld parameters are function of all three relative momenta. This corresponds to the modification of the effective screened nucleus, this degree of modification being dependent upon the momenta of the two particles. The effective charges of the $C^+(1s)$ core seen by the scattered electron and ejected electron are given, respectively, by

$$Z_{eff1} = Z_T - \frac{k_1}{k_{12}}\left[\frac{1}{2}\arccos(\hat{\mathbf{k}}_1 \cdot \hat{\mathbf{k}}_2)\right]^2\left(1 - \frac{|k_1 - k_2|}{4k_{12}}\right), \tag{17}$$

$$Z_{eff2} = Z_T - \frac{k_2}{k_{12}}\left[\frac{1}{2}\arccos(\hat{\mathbf{k}}_1 \cdot \hat{\mathbf{k}}_2)\right]^2\left(1 - \frac{|k_1 - k_2|}{4k_{12}}\right). \tag{18}$$

In this work, we will apply the present S3C method to the calculation of TDCS for *K*-shell electron-impact ionization of carbon.

The TDCS (including exchange) for the simultaneous detection of two continuum electrons escaping with momenta $\mathbf{k}_1$ and $\mathbf{k}_2$ and emerging into directions defined by solid angles Ω_1 and Ω_2 is given by

$$\frac{d^3\sigma}{d\Omega_1 d\Omega_2 dE_2} = 2(2\pi)^4 \frac{k_1 k_2}{k_i}\left[\frac{3}{4}|f(\mathbf{k}_1,\mathbf{k}_2) - g(\mathbf{k}_1,\mathbf{k}_2)|^2 + \frac{1}{4}|f(\mathbf{k}_1,\mathbf{k}_2) + g(\mathbf{k}_1,\mathbf{k}_2)|^2\right], \tag{19}$$

where E_2 being the energy of the ejected electron, $f(\mathbf{k}_1,\mathbf{k}_2)$ and $g(\mathbf{k}_1,\mathbf{k}_2)$ are the direct and exchange amplitudes, respectively, with $g(\mathbf{k}_1,\mathbf{k}_2) = f(\mathbf{k}_2,\mathbf{k}_1)$. The direct amplitude is

$$f(\mathbf{k}_1,\mathbf{k}_2) = \langle \Psi_f^- | V_i | \Psi_i^+ \rangle. \tag{20}$$

In order to account for the presence of two 1*s* electrons in the *K* shell of the target atom, we have multiplied the triple-differential cross section by a factor of 2.

The calculation has been done in the coplanar geometry, i.e., all the momentum vectors $\mathbf{k}_i$, $\mathbf{k}_1$, and $\mathbf{k}_2$ lie in the same plane. The calculation of $f(\mathbf{k}_1,\mathbf{k}_2)$ and $g(\mathbf{k}_1,\mathbf{k}_2)$ in Eq. (19) finally amounts to evaluating a three-dimensional integral which has been carried out numerically following the method described in our earlier work [15].

III. RESULTS AND DISCUSSIONS

We have computed the scattering amplitude, Eq. (20), with Ψ_f^- approximated by S3C, DS3C, and 3C wave function for inner-shell ionization of carbon atom by fast electron impact in coplanar and asymmetric geometry. The dynamical parameters are chosen in accordance with the relative measurements [1] performed on the C $\sigma 1s$ orbital of the C_2H_2 molecule. We adopt the convention that the angle of observation for the scattered electron is measured counterclockwise from the forward beam direction, while that for the ejected electron is measured clockwise.

The results are displayed in Figs. 1 and 2 where the present TDCS results have been plotted against the angle θ_2 of ejection of the slower electron. These figures also exhibit the corresponding experimental data together with the theoretical results due to Botero and Macek [7]. The data shown in Fig. 1(a) correspond to an incident energy $E_i = 1801.2$ eV, an energy of the ejected electron $E_2 = 9.6$ eV, and scattering angle $\theta_1 = -4°$ with a momentum transfer $|\mathbf{q}| = |\mathbf{k}_i - \mathbf{k}_1| = 1.255$ a.u. The data shown in Fig. 1(b) correspond to $E_i = 1832.4$ eV, $E_2 = 41$ eV, $\theta_1 = -5°$, and $|\mathbf{q}| = 1.457$ a.u. Solid lines correspond to the S3C results, the dash line to the 3C case, and the dash-dot line to the DS3C results. Figures 2(a) and 2(b) also display the corresponding TDCS results for some variants of the present model. The solid and dashed lines in both the figures correspond to the results computed from our general program by setting the parameter $\alpha_i = 0$ in Eq. (5), respectively. Keeping the interaction, Eq. (7), intact so that the perturbation V_i vanishes asymptotically. This amounts to replacing the initial channel Coulomb wave in Eq. (5) by a plane wave.

It should be noted that in all the kinematics presented here the energy of the scattered particle E_1 is kept fixed at

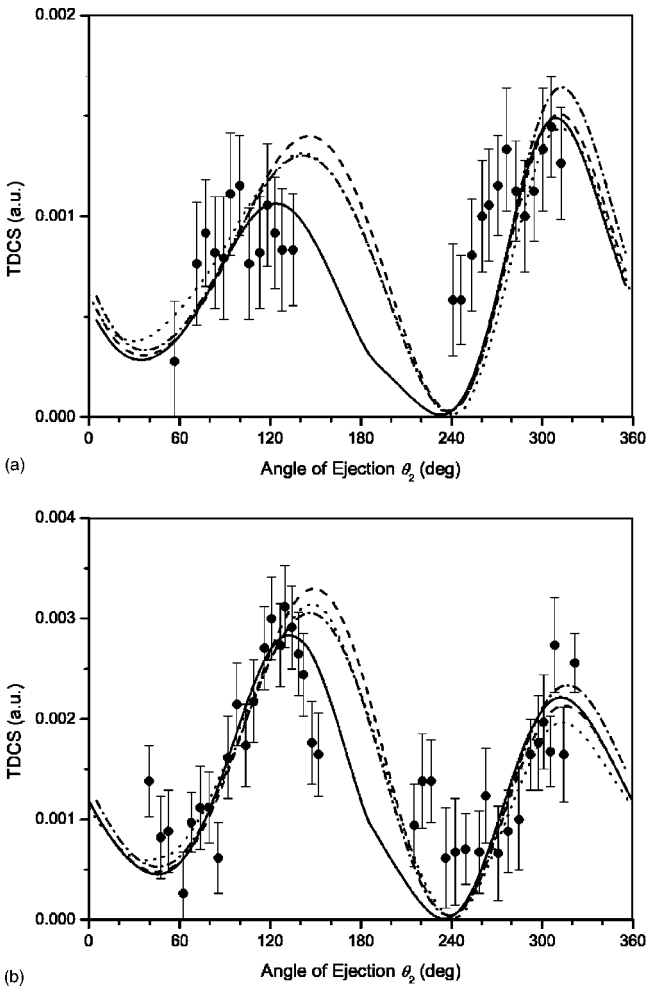

FIG. 1. Angular distribution of the TDCS for electron-impact ionization of carbon. Kinematical conditions: (a) incident energy $E_i=1801.2$ eV, ejected energy $E_2=9.6$ eV, and scattering angle $\theta_1=-4°$; (b) $E_i=1832.4$ eV, $E_2=41$ eV, $\theta_1=-5°$, as a function of θ_2. The solid line represents the S3C results, the dash-dotted line corresponds to the DS3C results, whereas the 3C calculations yield the dashed line, the dotted line is the results of Botero and Macek [7], and the circles are the experimental results from Ref. [1].

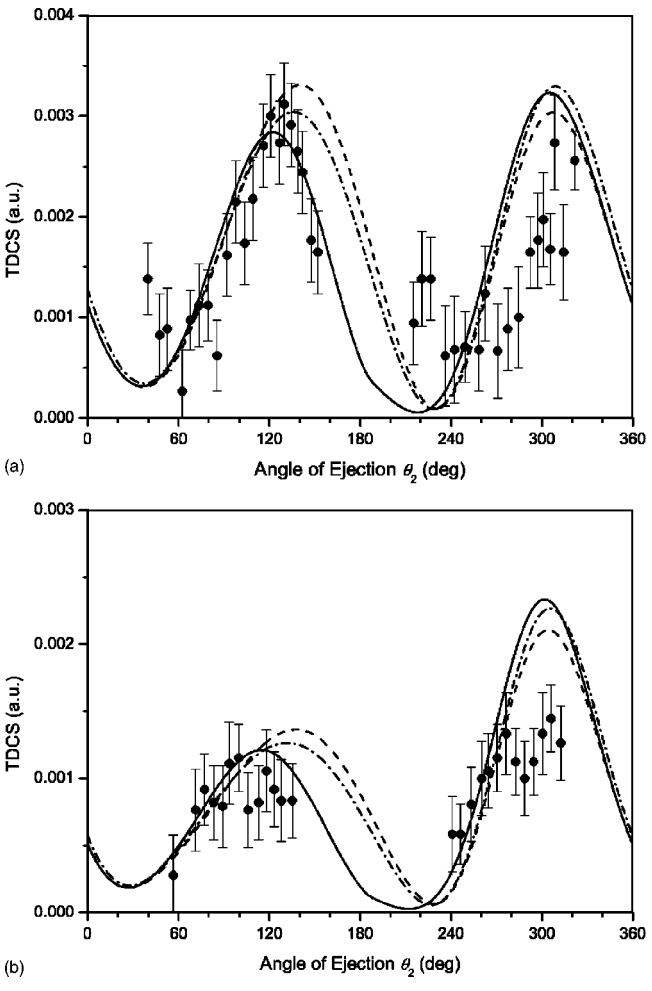

FIG. 2. The same kinematical condition as in Fig. 1, but the solid line, the dashed line, and the dash-dotted line represent the S3C, 3C, and DS3C results for incident plane wave [i.e., in Eq. (5) $\alpha_i=0$], respectively. The circles are the experimental results from Ref. [1].

1500 eV in Figs. 1 and 2. Since the measurement [1] is not absolute, we normalize the experimental data to the present calculations and consequently the comparison of the theoretical results with the experiment should be mainly qualitative.

Notice that the main feature of the TDCS is pointed out in Ref. [1], e.g., the presence of an intense recoil peak, which at $E_2=9.6$ eV is even larger than the binary one, is clearly reproduced in the theories. Since the recoil peak is mainly governed by the electron-nucleus interaction, the large recoil peak [Fig. 1(a)] may be qualitatively explained by strong elastic scattering from the nucleus [1]. This is an unusual feature for the outer-shell ionization of neutral atom at intermediate and high incident energies.

Although the qualitative feature of the experimental TDCS data is quite well described by the theories, the positions of the peaks is not well reproduced in the models. In fact the theoretical peak position is shifted towards larger ejection angles in both the cases (Fig. 1). As it may be seen from these figures that the S3C results are in better agreement with the experiment than those of the DS3C, 3C, and Botero and Macek's CBA [7], particularly in the S3C angular distribution for incident plane-wave (Fig. 2). We may easily deduce that the S3C model shows a large improvement over the DS3C, 3C, and CBA model in obtaining better magnitudes and shapes of the cross sections compared with the measurements.

However as far as the magnitude is concerned, the theoretical results are more or less within the experiment error bars from Fig. 1. The S3C results are found to be lower than the results of the DS3C, 3C, and CBA (Figs. 1 and 2), except in the backward direction, before the occurrence of binary peak. It is seen that, from Fig. 1, there are some difference among the results of the three theoretical models (i.e., 3C, DS3C, and CBA), in the present highly asymmetric kinematics. Near the recoil peak, the results of 3C are bigger than those of DS3C and the results of CBA are between those of DS3C and 3C. With increasing incident energy, the difference between the results of DS3C and CBA is diminishing. Near the binary peak, the results of DS3C are bigger than

those of 3C and the results of CBA are smaller than those of 3C. We remark that the DS3C results confirm the analysis made in Refs. [10,13,16,17] in that many-body coupling primarily affects the magnitude of the TDCS rather than its shape. In general, we note a satisfactory, although not perfect, agreement of the S3C results with experimental finding. This is readily concluded that, by comparing the DS3C, 3C, and S3C results, the merit of the S3C is the inclusion of the screening of the multielectron target which is neglected in the DS3C and 3C models.

Regarding the TDCS with the initial channel Coulomb wave replaced by a plane wave, it may be noted from Fig. 2 that the exact position of the peaks is very well reproduced in better accord with experiment than that predicted by DS3C, 3C, and CBA. From Fig. 2 it can be seen the binary peaks are overestimated but the recoil peaks are within the experiment error bars. The difference in magnitude between the results is minimum at the recoil peaks while the maximum occurs in the backward direction (i.e., in the binary region). This discrepancy increases with the decrease of impact energy. It demonstrates that the influence of the long-range Coulomb interaction in the initial channel is most prominent at lower incident energy [15], especially in the binary peak.

ACKNOWLEDGMENTS

This work was supported by the Natural Science Foundation of Shanxi Province (Grant No. 20001008) and the Science Foundation for Returnees of Shanxi Province [Grant Nos. (99)13 and (02)16] of China.

[1] L. Avaldi, R. Camilloni, and G. Stefani, Phys. Rev. A **41**, 134 (1990).
[2] A. Lahmam-Bennani, H. F. Wellenstein, A. Duguet, and A. Daoud, Phys. Rev. A **30**, 1511 (1984).
[3] G. Stefani, L. Avaldi, A. Lahmam-Bennani, and A. Duguet, J. Phys. B **19**, 3787 (1986).
[4] S. J. Cavanagh and B. Lohmann, Phys. Rev. A **57**, 2718 (1998).
[5] B. Lohmann, S. J. Cavanagh, M. A. Haynes, I. Taouil, A. Duguet, and A. Lahmam-Bennani, Aust. J. Phys. **51**, 679 (1998).
[6] X. Zhang, C. T. Whelan, H. R. J. Walters, R. J. Allan, P. Bickert, W. Hink, and S. Schönberger, J. Phys. B **25**, 4325 (1992).
[7] J. Botero and J. H. Macek, Phys. Rev. A **45**, 1541 (1992).
[8] B. Nath, R. Biswas, and C. Sinha, Z. Phys. D: At., Mol. Clusters **42**, 157 (1997).
[9] M. Brauner, J. S. Briggs, and H. Klar, J. Phys. B **22**, 2265 (1989).
[10] J. Berakdar and J. S. Briggs, Phys. Rev. Lett. **72**, 3799 (1994).
[11] A. Dutta, B. Nath, and C. Sinha, Phys. Rev. A **64**, 041214 (2001).
[12] F. Maulbetsch and J. S. Briggs, J. Phys. B **26**, 1679 (1993).
[13] J. Berakdar, J. S. Briggs, I. Bray, and D. V. Fursa, J. Phys. B **32**, 895 (1999).
[14] Z. J. Chen, Q. C. Shi, S. M. Zhang, J. Chen, and K. Z. Xu, Phys. Rev. A **56**, R2514 (1997).
[15] X. F. Jia, Q. C. Shi, Z. J. Chen, J. Chen, and K. Z. Xu, Phys. Rev. A **55**, 1971 (1997).
[16] J. Berakdar, J. Röder, J. S. Briggs, and H. Ehrhardt, J. Phys. B **29**, 6023 (1996).
[17] J. Berakdar, Phys. Rev. A **56**, 370 (1997).